Linear stability of buoyant convection in a horizontal layer of an electrically conducting fluid in moderate and high vertical magnetic field

A. Hudoba,[1, a)] S. Molokov,[1] S. Aleksandrova,[2] and A. Pedcenko[1]
[1)] *School of Computing, Electronics and Mathematics, Coventry University, Priory Street, Coventry CV1 5FB, United Kingdom*
[2)] *School of Mechanical, Aerospace and Automotive Engineering, Coventry University, Priory Street, Coventry CV1 5FB, United Kingdom*

(Dated: 9 June 2016)

Linear stability of buoyant convective flow in a horizontal layer of an electrically conducting fluid is considered with reference to horizontal Bridgman semiconductor crystal growth. The fluid flows owing to the horizontal temperature gradient in the presence of a vertical magnetic field. The main interest here is in the stability of the flow for a sufficiently strong magnetic field, for the Hartmann number $Ha > 10$, and increasing to high values, of the order of $10^3 - 10^4$. The Prandtl number, Pr, has been fixed at $Pr = 0.015$. It is shown that besides the Hartmann number the instability strongly depends on the type of the thermal boundary conditions at the horizontal walls. For thermally conducting walls the basic temperature profile exhibits zones of unstable thermal stratification, which leads to instabilities owing to the Rayleigh-Bénard mechanism. However, the transitions between various, most unstable modes as Ha increases is not trivial. For sufficiently high values of Ha the most unstable mode consists of transverse oscillatory rolls located in the region of unstable stratification. For thermally insulating walls, the transitions are simpler, and for sufficiently high Ha the most unstable mode consists of longitudinal, steady, three-dimensional mode which is concentrated in the Hartmann layers at the horizontal boundaries. This mode has a combined dynamic-thermal origin and is owed to a strong shear in the Hartmann layers. The electrical boundary conditions do not qualitatively affect the picture of transitions between modes for both thermally conducting and thermally insulating walls.

I. INTRODUCTION

Buoyant convection of electrically conducting fluids in the presence of a magnetic field is important for such applications as semiconductor crystal growth[1] and liquid metal blankets for tokamaks[2]. Concerning the crystal growth, convection is primarily responsible for striations in grown crystals of semiconducting materials, such as silicon, which adversely affect reliability of semiconductor chips. One of the possible solutions to reduce striations is to apply a sufficiently high magnetic field which would damp convective motion within the melt. The efficiency of damping depends not only on the direction of the applied magnetic field and its strength, but also on the type of instabilities that survive magnetic damping.

While for low magnetic field certain knowledge of the nature of instabilities exists, for moderate to high field there have been very few studies. Here we will be dealing with one of the most fundamental problems for which full understanding is still lacking. This is linear stability of a convective flow of an electrically conducting, incompressible fluid in an infinite layer between horizontal solid walls (Fig. 1). The fluid flows owing to a constant, imposed temperature gradient in the $-x-$direction in the presence of a uniform magnetic field $\mathbf{B}$ applied vertically, in the $z-$direction (x, y, z are Cartesian co-ordinates with the origin of the co-ordinate system placed at mid-height of the layer).

For low values of the Hartmann number, Ha, which characterizes the ratio of the electromagnetic to viscous forces, linear stability studies do exist[3,4]. It has been shown that for $Ha \lesssim 10$ and for low values of the Prandtl number, Pr, which is typical for molten semiconductors, the flow is unstable to two-dimensional perturbations in the (x, z)-plane. These perturbations are rolls with axes transverse to both the imposed temperature gradient and magnetic field. The rolls are stationary and are related to the existence of the inflection point in the basic velocity profile at $z = 0$, which is also the point where the two counterflows meet. Stationary transverse rolls are highly, exponentially damped by the field as the shear in the core tends to become a constant, Couette-flow-like, and the inflection point is eliminated. For $Ha \gtrsim 10$ these instabilities disappear.

[a)] ac0640@coventry.ac.uk

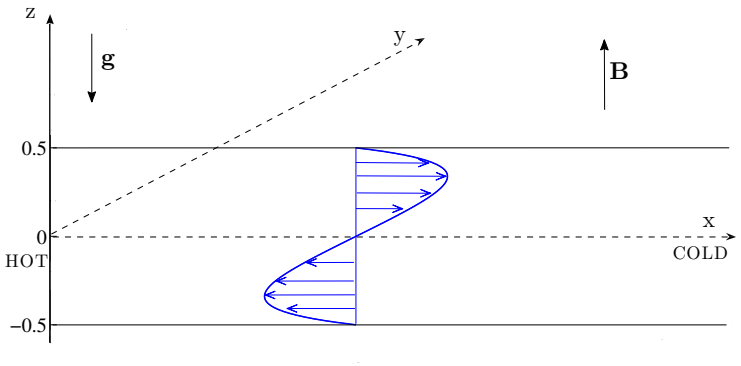

FIG. 1. Schematic diagram of horizontal circulation in buoyancy-driven convection in an infinite horizontal layer with an axial temperature gradient and a vertical magnetic field.

It was found that for higher values of Ha the transverse rolls give way to longitudinal rolls aligned with the imposed temperature gradient, and which have thermal origin. The value of Ha for which transitions between modes occurs depends on the value of the Prandtl number.

Here we focus on the case of moderate and high magnetic fields ($Ha \gtrsim 10$) and present the results of numerical analysis. It is shown that besides the values of the dimensionless parameters, the instability strongly depends on the thermal boundary conditions. The cases of thermally conducting or insulating boundaries are discussed in Sections V and VI, respectively. The electrical boundary conditions do not qualitatively change the instability patterns, but the quantitative results are presented in Tables III-IV and VI-VII. In previous studies the main emphasis was on the investigation of variation of the Prandtl number for several values of Ha. Here we fix the Prandtl number at $Pr = 0.015$, which corresponds to Indium Phosphide and which is typical for liquid metals and molten semiconductors. Preliminary results for $Pr = 0.01$ have been presented at a conference[5].

II. FORMULATION

Consider buoyancy-driven flow of a viscous, electrically conducting liquid of density ρ, kinematic viscosity ν, thermal conductivity κ and electric conductivity σ filling a horizontally unbounded gap between two parallel walls, which are separated by the distance d (Fig. 1). The fluid density varies with temperature T as $\rho = \rho_0(1-\beta(T-T_0))$, where β is the thermal expansion coefficient, T_0 is a reference temperature and ρ_0 is the corresponding density. The boundaries can be either thermally and electrically insulating or perfectly conducting, which gives four combinations of the boundary conditions. A constant, horizontal temperature gradient τ is imposed along the layer. In a laboratory implementation, two distant opposite vertical boundaries are set at different temperatures and the fluid is driven upward near the hot and downward near the cold wall. Owing to the induced pressure gradient this causes a horizontal steady buoyancy-driven circulation due to thermal expansion of the liquid. The flow is subjected to a uniform, vertical magnetic field $\mathbf{B} = B_0\mathbf{e}_z$.

All variables are made dimensionless using the depth d as the length scale, while the time t, the magnetic field, the fluid velocity $\mathbf{v} = (u, v, w)$, the pressure p, the temperature difference $T - T_0$, the electric potential ϕ, and the electric current $\mathbf{j}$ are scaled with d^2/ν, B_0, ν/d, $\rho_0\nu^2/d^2$, τd, $B_0\nu$, and $B_0\sigma\nu/d$, respectively. In liquid metals and molten semiconductors the magnetic Prandtl number $Pr_m = \mu_0\sigma\nu$, is very small, typically of order $10^{-5} - 10^{-7}$. Here μ_0 is the magnetic permeability of vacuum. Therefore we use the so-called quasi-static approximation whereby the induced magnetic field is neglected[2]. Then the dimensionless governing equations in the Boussinesq approximation are (e.g. Ref. 3):

$$\frac{\partial \mathbf{v}}{\partial t} + (\mathbf{v}\cdot\nabla)\mathbf{v} = -\nabla p + \nabla^2\mathbf{v} + Ha^2\mathbf{j}\times\mathbf{e}_z + GrT\hat{e}_z \ , \tag{1}$$

$$\mathbf{j} = -\nabla\phi + \mathbf{v}\times\mathbf{e}_z \ , \tag{2}$$

$$\frac{\partial T}{\partial t} + (\mathbf{v}\cdot\nabla)T = \frac{1}{Pr}\nabla^2 T \ , \tag{3}$$

$$\nabla \cdot \mathbf{v} = 0 \ , \tag{4}$$

$$\nabla \cdot \mathbf{j} = 0 \ . \tag{5}$$

Here the dimensionless parameters, $Ha = B_0 d\sqrt{\sigma/(\rho_0 \nu)}$, $Gr = g\beta\tau d^4/\nu^2$ and $Pr = \nu/\kappa$, are the Hartmann, Grashof and Prandtl numbers, respectively, where g is the gravitational acceleration.

The boundary condition for fluid velocity is the no-slip condition:

$$\mathbf{v} = 0 \text{ at } z = \pm 1/2 \ . \tag{6}$$

The electrical boundary conditions are either

$$\phi = 0 \text{ at } z = \pm 1/2 \tag{7}$$

for perfectly electrically conducting walls, or

$$\frac{\partial \phi}{\partial z} = 0 \text{ at } z = \pm 1/2 \tag{8}$$

for perfectly insulating walls.

The thermal boundary conditions are either

$$T = -x \text{ at } z = \pm 1/2 \tag{9}$$

for thermally conducting walls, or

$$\frac{\partial T}{\partial z} = 0 \text{ at } z = \pm 1/2 \tag{10}$$

for thermally insulating walls.

III. BASIC FLOW AND DISTURBANCES

The system of equations with the boundary conditions above admits a steady, parallel flow solution, called the basic flow and is denoted by an overbar, with

$$\overline{u}(z) = -\overline{j}_y(z) = \overline{Gr} \left\{ z - \frac{\sinh(Haz)}{2\sinh(Ha/2)} \right\}, \tag{11}$$

$$\overline{T}(x,z) = -x + \overline{Ra} \left\{ -\frac{1}{6} z^3 + Cz + \frac{\sinh(Haz)}{2Ha^2 \sinh(Ha/2)} \right\}, \tag{12}$$

$$\overline{\phi}(z) = 0 \ , \tag{13}$$

$$\overline{p}(x,z) = -Gr\, x\, z \ . \tag{14}$$

Here $\overline{Gr} = GrHa^{-2}$, $\overline{Ra} = RaHa^{-2}$, where $Ra = GrPr$ is the Rayleigh number. The constant C in the expression for temperature is:

$$C = \frac{1}{24} - \frac{1}{Ha^2}$$

for thermally conducting walls or

$$C = \frac{1}{8} - \frac{\coth(Ha/2)}{2Ha}$$

for thermally insulating walls.

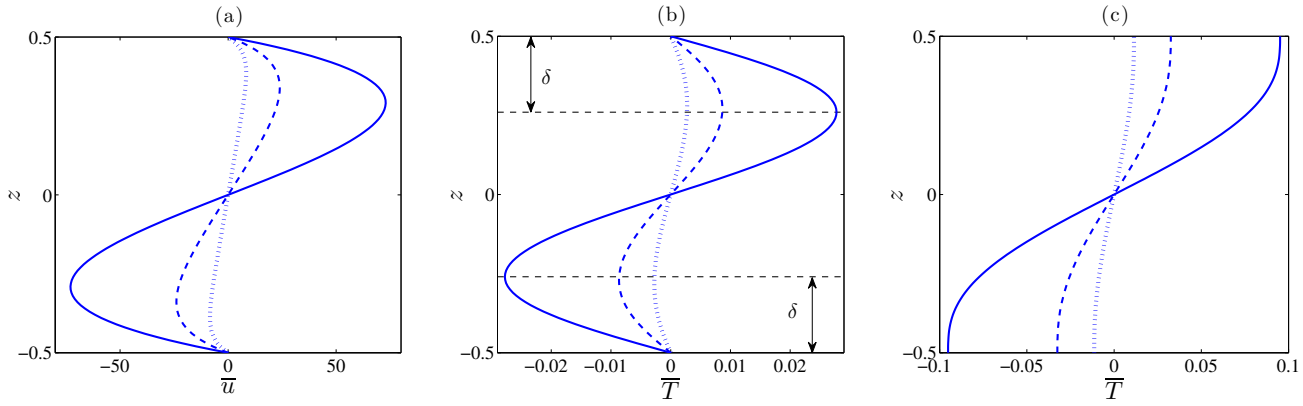

FIG. 2. Basic velocity (a) and temperature for thermally conducting walls (b), and for thermally insulating walls (c). Here $Gr = 10^4$, $Pr = 0.015$, and $Ha = 2$ (solid line), $Ha = 10$ (broken line), $Ha = 20$ (dotted line). For thermally conducting walls unstable thermal stratification zones near the horizontal boundaries are denoted by δ.

The basic flow velocity and temperature profiles for this magnetohydrodynamic (MHD) flow[6] may also be obtained from the corresponding solution for a vertical layer in the horizontal magnetic field with differentially heated walls[7] using an appropriate change of variables. Typical velocity and temperature profiles for the basic flow are shown in Fig. 2.

It should be noted that first of all, in the expression for $\overline{p}$ an additive function of z only has been neglected as it affects neither the basic flow nor the disturbances. Secondly, the electric potential $\overline{\phi}$ is equal to zero for both electrically conducting and insulating walls because the current induced in the $y-$direction is antisymmetric. It closes the loop at $y \to \pm\infty$ fully within the fluid between the part of the layer for $z > 0$ and $z < 0$ in a symmetric way, not entering the walls. Thirdly, as $\overline{\phi} = 0$, the Lorentz force $Ha^2\,\overline{j}_y \mathbf{e}_x = -Ha^2\,\overline{u}\,\mathbf{e}_x$ reduces to simple damping at every point within the flow.

For $Ha \gg 1$, the region of highest interest here, neglecting exponentially decaying terms with Ha, the basic fluid velocity and temperature have the following asymptotics:

$$\overline{u}(z) \cong \overline{Gr}\left\{z - \frac{1}{2}\left[e^{Ha(z-1/2)} - e^{-Ha(z+1/2)}\right]\right\}, \tag{15}$$

$$\overline{T}(x,z) \cong -x + \overline{Ra}\left\{\left[-\frac{1}{6}z^3 + Cz\right] + \frac{1}{2Ha^2}\left[e^{Ha(z-1/2)} - e^{-Ha(z+1/2)}\right]\right\}, \tag{16}$$

where $C = \frac{1}{24} - Ha^{-2}$ for thermally conducting walls or $C \cong \frac{1}{8} - 0.5Ha^{-1}$ for thermally insulating walls. These asymptotic expressions are used for calculations here for $Ha > 100$.

It is seen from Eqs. (15) and (16) that for $Ha \gg 1$ the flow consists of the core given by the first terms and the exponential Hartmann layers of thickness $O(Ha^{-1})$ at both walls. The core velocity is equal to $\overline{Gr}\,z$, i.e. in most part of the fluid the flow becomes Couette-like.

We are interested in critical values of parameters for which the basic flow loses stability. Every scalar and vector function f is represented as a sum of the basic flow component and disturbance as follows:

$$f(x,y,z,t) = \overline{f} + \hat{f}(z)\exp\left(ixk_x + iyk_y + \lambda t\right), \tag{17}$$

where k_x, k_y are components of the wavenumber vector $\mathbf{k} = k_x\mathbf{e}_x + k_y\mathbf{e}_y$ and λ is a complex growth rate. The disturbance for temperature is denoted as $\widehat{\theta}(z)\exp\left(ixk_x + iyk_y + \lambda t\right)$.

To derive the disturbance equations, first Eq. (17) is substituted into Eqs. (1)$-$(5) for each flow variable, and quadratic disturbance terms are neglected. Next, the disturbance vorticity, $\widehat{\omega} = \text{curl}\,\widehat{\mathbf{v}}$ is introduced, and the disturbance pressure, current, and $x-$ and $y-$ components of the disturbance velocity are eliminated from the equations. This is done by applying double curl to Eq. (1), div to Eq. (2) and using Eqs. (4) and (5). The resulting disturbance equations are:

$$\{\mathbf{D}^4 - \overline{u}ik_x\mathbf{D}^2 + \overline{u}''ik_x - Ha^2\frac{d^2}{dz^2}\}\hat{w} - Gr\mathbf{k}^2\hat{\theta} = \lambda\mathbf{D}^2\hat{w}, \tag{18}$$

$$\{\mathbf{D}^2 - \overline{u}ik_x - Ha^2\}\hat{\omega}_z + \overline{u}'ik_y\hat{w} - Ha^2\mathbf{k}^2\hat{\phi} = \lambda\hat{\omega}_z, \tag{19}$$

$$\{\frac{1}{Pr}\mathbf{D}^2 - \overline{u}ik_x\}\hat{\theta} + i\frac{k_y}{\mathbf{k}^2}\hat{\omega}_z - \{\overline{\theta}' - i\frac{k_x}{\mathbf{k}^2}\frac{d}{dz}\}\hat{w} = \lambda\hat{\theta}, \tag{20}$$

$$\hat{\omega}_z = \mathbf{D}^2\hat{\phi}, \tag{21}$$

where $' = d/dz$ and $\mathbf{D} = \mathbf{e}_z\frac{d}{dz} + i\mathbf{k}$. These equations are for the normal to the walls components of velocity and vorticity, temperature and electric potential.

The boundary conditions for the normal velocity and vorticity are:

$$\hat{w} = \hat{w}' = \hat{\omega}_z = 0 \quad \text{at} \quad z = \pm 1/2. \tag{22}$$

The thermal boundary conditions are:

$$\hat{\theta} = 0 \quad \text{at} \quad z = \pm 1/2 \tag{23}$$

for thermally conducting walls, or

$$\hat{\theta}' = 0 \quad \text{at} \quad z = \pm 1/2 \tag{24}$$

for thermally insulating walls.

The electrical boundary conditions are:

$$\hat{\phi} = 0 \quad \text{at} \quad z = \pm 1/2 \tag{25}$$

for electrically conducting walls, or

$$\hat{\phi}' = 0 \quad \text{at} \quad z = \pm 1/2 \tag{26}$$

for electrically insulating walls.

The disturbance equations with four combinations of the boundary conditions have been solved numerically with the Chebyshev spectral collocation method using Matlab. The code is an extension of the matrix differentiation suite developed by Weideman and Reddy[8]. The code has been tested on various known solutions for the hydrodynamic and MHD stability problems. The agreement in all the cases is excellent. Between 20 and 180 Chebyshev polynomials have been used to solve the disturbance equations depending on the value of the Hartmann number. High number of polynomials is required to properly resolve the thin Hartmann layers at the walls, especially for the case of thermally insulating walls as we will see below.

IV. ENERGY ANALYSIS

Energy analysis for disturbances is performed as in Kaddeche et al.[3] We reproduce only the final expressions for the energy components. In the equations below quantities with an asterisk denote complex conjugate functions.

Concerning the equation of motion (1), the rate of change of the fluctuation kinetic energy is denoted with K:

$$\mathrm{Re}(\partial_t K) = \mathrm{Re}(\lambda)\int_z \hat{\mathbf{v}}\cdot\hat{\mathbf{v}}^* dz = K_d + K_f + K_b + K_m \ , \tag{27}$$

with the following terms:
the viscous dissipation of fluctuating kinetic energy K_d :

$$K_d = \mathrm{Re}\left(\int_z \mathbf{D}^2\,\hat{\mathbf{v}}\cdot\hat{\mathbf{v}}^* dz\right) \ , \tag{28}$$

the production of fluctuating kinetic energy by shear of mean flow K_f :

$$K_f = -\mathrm{Re}\left(\int_z \overline{u}'\,\hat{w}\,\hat{u}^* dz\right) \ , \tag{29}$$

the production of fluctuating kinetic energy by buoyancy forces K_b :

$$K_b = \mathrm{Re}\left(\int_z Gr\,\hat{\theta}\,w^*)dz\right) \ , \tag{30}$$

the dissipation of fluctuating kinetic energy by magnetic forces K_m :

$$K_m = \mathrm{Re}\left(\int_z Ha^2(ik_x\hat{\phi}\,\hat{v}^* - ik_y\hat{\phi}\,\hat{u}^* - \hat{u}\,\hat{u}^* - \hat{v}\,\hat{v}^*)dz\right) \ . \tag{31}$$

For the energy equation (3), the rate of change of the fluctuation thermal energy Θ is:

$$\mathrm{Re}(\partial_t\Theta) = \mathrm{Re}(\lambda)\int_z \hat{\theta}\,\hat{\theta}^* dz = \Theta_d + \Theta_1 + \Theta_2 \ , \tag{32}$$

with the dissipation of fluctuating thermal energy Θ_d :

$$\Theta_d = \mathrm{Re}\left(\int_z \frac{1}{Pr}\mathbf{D}^2\,\hat{\theta}\cdot\hat{\theta}^* dz\right) \ , \tag{33}$$

the production of fluctuating thermal energy by vertical transport of temperature Θ_1 :

$$\Theta_1 = -\mathrm{Re}\left(\int_z \overline{T}'\hat{w}\,\hat{\theta}^* dz\right) \ , \tag{34}$$

the production of fluctuating thermal energy by horizontal transport of temperature Θ_2 :

$$\Theta_2 = \mathrm{Re}\left(\int_z \hat{u}\,\hat{\theta}^* dz\right) \ . \tag{35}$$

The negative values of energy contributions characterize stabilizing terms, while the positive contributions are destabilizing. Some of the terms may change the sign depending on the value of parameters and the boundary conditions.

In the problems considered here the energy results are given at the critical threshold $\mathrm{Re}(\lambda) = 0$. Since the critical eigenvectors are defined to within a multiplicative constant, the energy equations specific terms also can be given to within a multiplicative constant. In order to present well-defined energy balances, the energy equations are scaled by the corresponding dissipation terms:

$$\bar{K}_d = \bar{K}_f + \bar{K}_b + \bar{K}_m = 1 \ , \tag{36}$$

$$\bar{\Theta}_d = \bar{\Theta}_1 + \bar{\Theta}_2 = 1 \ , \tag{37}$$

where the scaled terms are denoted with an overbar.

To compare the kinetic and thermal energy dissipation, the following dimensionless ratio is given:

$$R_d = \frac{1}{Gr}\frac{K_d}{\Theta_d} \ . \tag{38}$$

V. RESULTS FOR THERMALLY CONDUCTING WALLS

For thermally conducting walls there are three main sources of instability. Two of them are of dynamic origin and one is thermal. For low Ha the first dynamic source of instability appears. This is caused by the inflection line in the basic velocity profile[3]. This mode, taking the forms of stationary, two-dimensional, transverse rolls centred at $z = 0$, is highly damped by the increasing magnetic field and vanishes at about $Ha \sim 10$. The second source of dynamic origin could lead to the oscillatory rolls related to the instability of the Hartmann layers[9] of the basic profile. Finally, for thermally conducting walls the thermal mode has the origin in the two thermal stratification zones located at the upper and lower parts of the layer (see Fig. 2b). This leads to oscillatory three-dimensional modes with axes parallel to the basic flow[3]. We show here, however, that these modes may not be the most unstable depending on the value of the Hartmann number. Mathematically, $k_y = 0$ for transverse modes, and $k_x = 0$ for longitudinal modes.

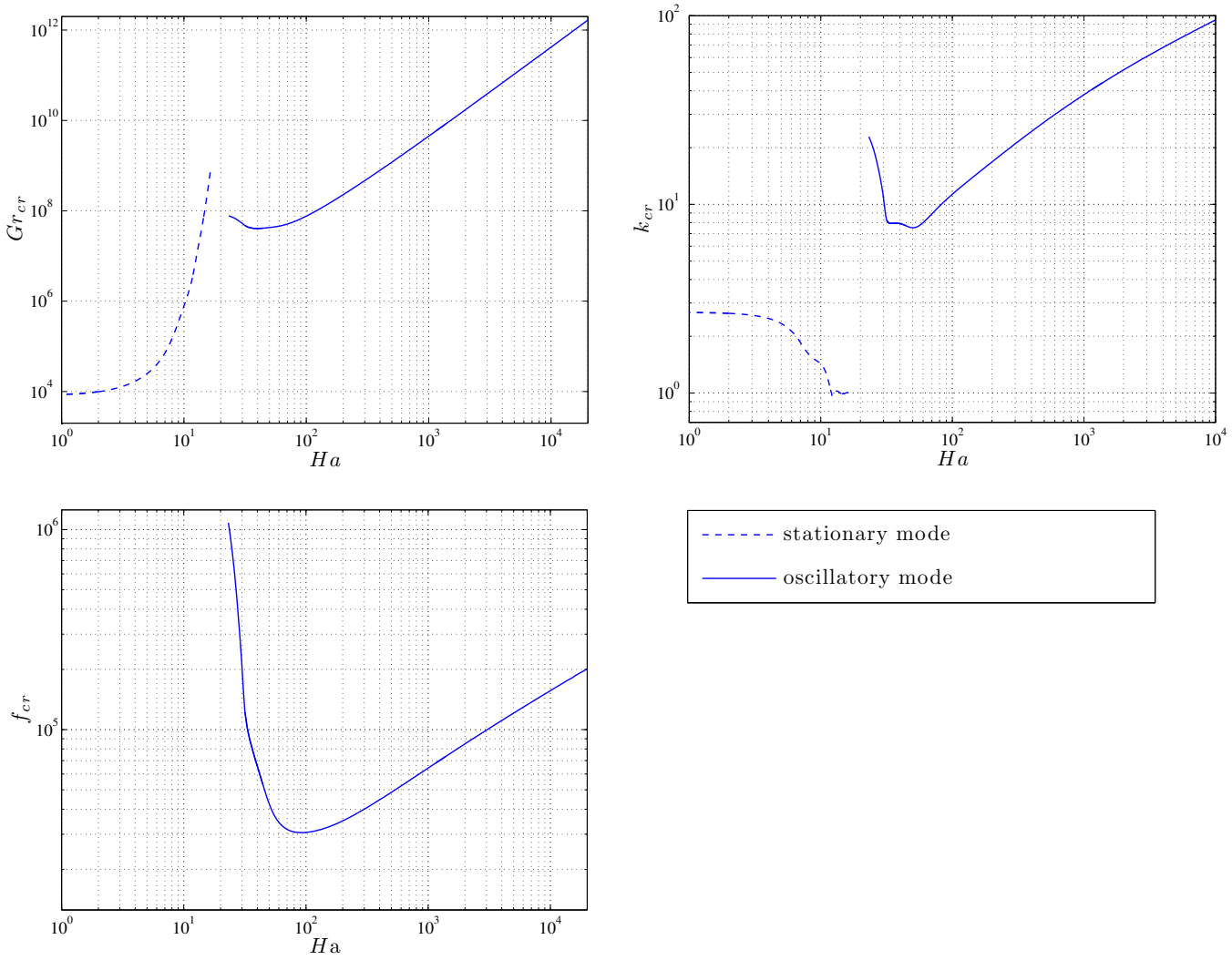

FIG. 3. Critical values of parameters for thermally conducting walls, transverse modes.

A. Transverse modes

The electrical boundary conditions have no effect on the transverse instabilities as the corresponding disturbance current does not enter the walls, similarly to the basic flow. The stationary mode of dynamic origin remains the dominant instability for low Ha and disappears for $Ha \approx 16$ (Fig. 3). New, previously undiscovered, oscillatory mode appears at a higher value of the Hartmann number, $Ha \approx 29$. Contour plots of disturbed temperature isotherms and velocity streamlines (Fig. 4) show clearly, that these instabilities are located near the horizontal boundaries, indicating their thermal origin. There are two such instability modes located in the upper and lower parts of the layer, respectively. They correspond to two different eigenvalues with equal real parts. The two resulting waves propagate to the right (Fig. 4, upper graphs) and to the left (Fig. 4, lower graphs), being carried by the basic flow in these two opposite directions.

For the new mode, after a short decrease of Gr_{cr} with the increasing Ha, further increase of the magnetic field strength shifts the instability onset to higher Grashof numbers. The wavenumbers rapidly increase up to high values, indicating a strong decrease of the size of the marginal cells. The reason for this will be discussed below. The frequency rapidly decreases before reaching its minimum at $Ha \approx 91.4$ and then increases steadily with increasing Ha. For highest values of $Ha \sim 10^4$ reached here, the critical values of parameters reach asymptotic relations $Gr_{cr} \cong 4550\, Ha^{1.99}$, $k_{cr} \cong 3.76\, Ha^{0.35}$ and $f_{cr} \cong 5435\, Ha^{0.36}$, which are close to: $Gr_{cr} \cong 4155\, Ha^2$, $k_{cr} \cong 4.45\, Ha^{1/3}$ and $f_{cr} \cong 7395\, Ha^{1/3}$. This scaling appears because the instabilities are driven essentially by the Rayleigh-Bénard mechanism[10].

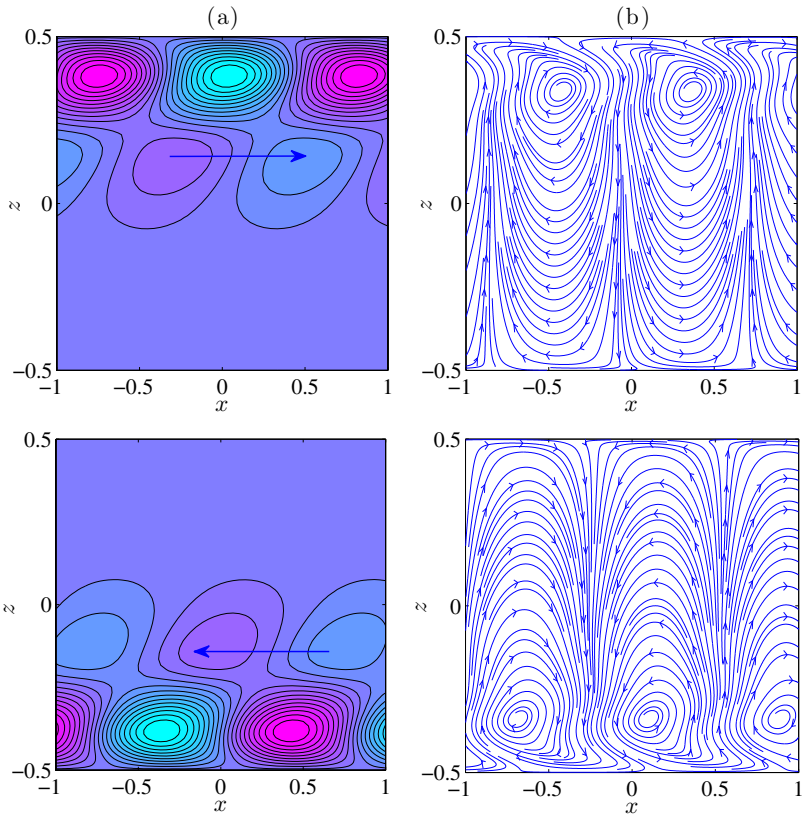

FIG. 4. Disturbance of temperature (a) and streamfunction (b) for the thermal transverse mode and for $Ha = 60$.

TABLE I. Energy balance for thermally conducting walls for increasing values of Ha: transverse modes.

Ha	$\overline{K}_f$	$\overline{K}_b$	$\overline{K}_m$	$\overline{\Theta}_1$	$\overline{\Theta}_2$	R_d
stationary instabilities						
2	1.08	-0.03	-0.05	0.06	0.94	25.48
6	1.48	-0.11	-0.37	0.14	0.86	6.67
10	1.87	-0.54	-0.33	0.73	0.27	0.53
oscillatory instabilities						
60	-0.90	4.36	-2.46	0.99	0.01	0.05
100	-1.63	9.19	-6.56	0.93	0.07	0.03
200	-1.16	16.21	-14.05	0.92	0.08	0.02
500	-0.32	23.91	-22.59	0.96	0.04	0.01
1000	-0.10	30.87	-29.77	0.97	0.03	0.01

The results for energy balances for increasing values of Ha are summarized in Table I. The thermal energy balance is strongly modified by the increasing magnetic field strength, even at low values of Ha. Both terms corresponding to the production of fluctuating thermal energy by vertical and horizontal transport of temperature are positive, indicating destabilizing effects. At values of Ha just before the disappearance of the stationary instabilities the vertical transport of temperature contribution becomes the main destabilizing term.

For the oscillatory mode the thermal energy balance is dominant and is not strongly modified by the increasing magnetic field strength. The vertical transport of temperature represented by the term $\overline{\Theta}_1$ is the main destabilizing contribution, while the destabilizing effect of the horizontal transport of temperature, given by $\overline{\Theta}_2$, is very weak.

In the kinetic energy balance the only destabilizing contribution comes from buoyancy. The term $\overline{K}_b$ increases with increasing Ha, while the dissipation of fluctuating kinetic energy by magnetic forces, $\overline{K}_m$, is the dominant stabilizing effect. Thus in the momentum equation, buoyancy-magnetic balance prevails, which is important for high$-Ha$ asymptotics.

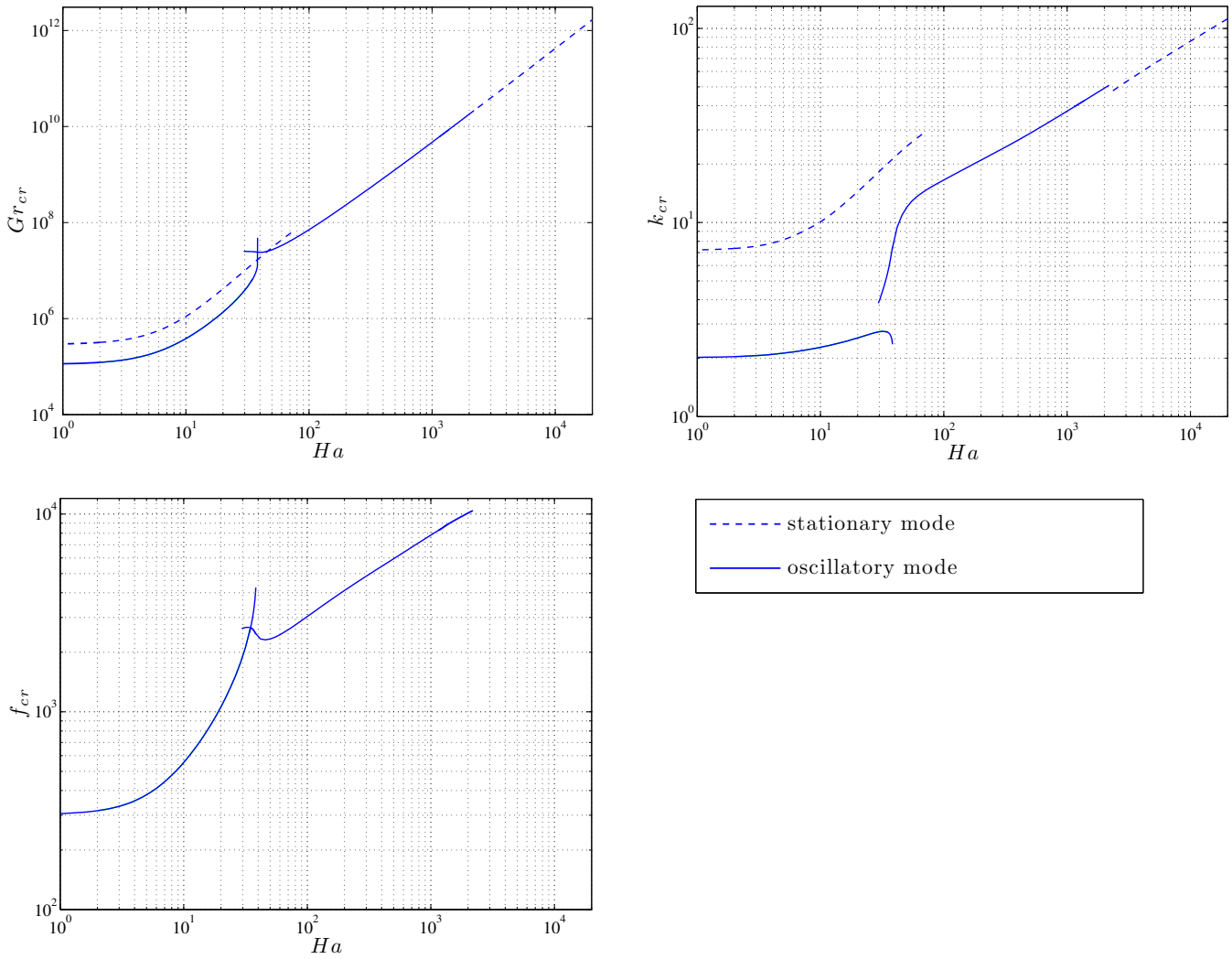

FIG. 5. Critical values of parameters for thermally conducting and electrically insulating walls, longitudinal modes.

B. Longitudinal modes

For the three-dimensional, oscillatory, longitudinal modes, increasing the magnetic field strength shifts the onset of the instabilities to higher Grashof numbers very rapidly (Fig. 5). For $Ha \approx 38$ the first branch of the oscillatory longitudinal mode reaches its limiting value before its disappearance. The wavenumber remains almost constant, insignificantly increasing and reaching its maximum $k_y \approx 2.75$ at $Ha \approx 31.7$. The critical frequency increases rapidly before the mode's disappearance.

New, stationary longitudinal mode is more stable at the lowest Hartmann number values but for $38 < Ha < 46$ it becomes the dominating instability of longitudinal type.

A new oscillatory mode appears at $Ha \approx 33$ and for $Ha > 46$ is the most unstable longitudinal mode, with critical parameter values steadily increasing with the increasing Ha. For this second oscillatory branch, after a slight decrease, the critical frequency increases monotonically with increasing Ha. However, for $Ha \approx 2180$, the frequency drops to zero, and the instability changes to a stationary mode. This is accompanied by a drop in the value of the wavenumber from $k_y \approx 51$ to $k_y \approx 47.8$. However, the critical value of the Grashof number does not exhibit any jumps.

For this stationary mode, and for high values of the Hartmann number, $Ha \sim 10^4$, the critical values reach the following asymptotic: $Gr_{cr} \cong 4914\, Ha^{1.98}$ and $k_{cr} \cong 2.28\, Ha^{0.39}$. If the exponents of Ha are fixed to 2 and 1/3, respectively, the asymptotics become $Gr_{cr} \cong 4189\, Ha^2$ and $k_{cr} \cong 3.95\, Ha^{1/3}$. It is worth noting that these values are close to the exact asymptotics obtained in Ref. 5.

For the *oscillatory* longitudinal instabilities at high Ha, the dominant thermal energy balance shows that the

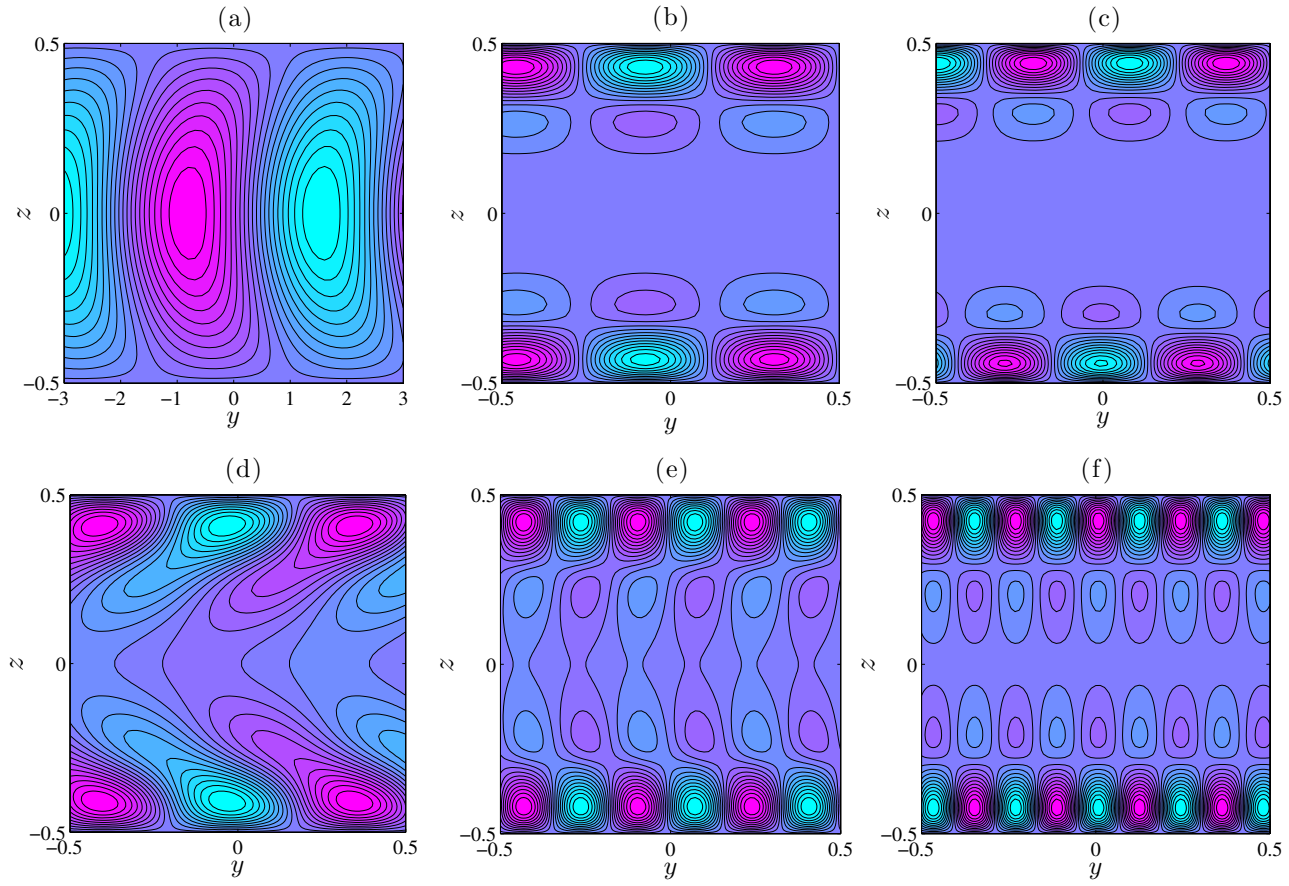

FIG. 6. Disturbance of temperature for the longitudinal oscillatory mode and for $Ha = 25$ ($f_{cr} = 1415.3$) (a), the longitudinal stationary mode for $Ha = 25$ (b), $Ha = 40$ (c), and the high Ha thermal branch (bottom row) for $Ha = 100$ ($f_{cr} = 3033.7$) (d), $Ha = 1000$ ($f_{cr} = 7820.5$) (e), $Ha = 3000$ ($f_{cr} = 0$) (f). Thermally conducting and electrically insulating walls.

TABLE II. Energy balance for thermally conducting and electrically insulating walls for increasing values of Ha: longitudinal modes.

Ha	$\overline{K}_f$	$\overline{K}_b$	$\overline{K}_m$	$\overline{\Theta}_1$	$\overline{\Theta}_2$	R_d
oscillatory instabilities						
2	1.02	0.04	-0.06	-0.01	1.01	0.42
10	2.01	0.35	-1.36	-0.04	1.04	0.14
25	3.09	2.71	-4.80	-0.15	1.15	0.06
stationary instabilities						
2	1.01	0.00	-0.01	0.10	0.90	8.69
10	1.12	0.01	-0.13	0.19	0.81	5.43
25	1.29	0.02	-0.31	0.44	0.56	3.17
60	1.64	0.09	-0.73	0.98	0.02	1.21
oscillatory instabilities						
60	2.79	0.60	-2.39	0.67	0.33	0.20
100	2.26	1.83	-3.09	0.84	0.16	0.11
200	1.31	5.16	-5.47	1.02	-0.02	0.06
500	0.57	14.96	-14.53	1.06	-0.06	0.02
1000	0.29	27.58	-26.87	1.05	-0.05	0.01
stationary instabilities						
3000	0.09	78.86	-77.95	1.03	-0.03	0.005
5000	0.04	101.42	-100.46	1.02	-0.02	0.004

production of fluctuating thermal energy by the vertical transport of temperature $\overline{\Theta}_1$ is here the main destabilizing effect. The production of energy by the horizontal transport of temperature $\overline{\Theta}_2$ serves as a secondary destabilizing contribution at the appearance of the instability. It quickly decreases with increasing Ha and for $Ha \approx 200$, becomes a weak stabilizing contribution.

In the kinetic energy balance, again both effects due to shear of mean flow $\overline{K}_f$ and buoyancy forces $\overline{K}_b$ are destabilizing. Here the first contribution, $\overline{K}_f$, decreases rapidly with increasing Ha and the buoyancy term $\overline{K}_b$ becomes the main destabilizing contribution, growing quickly with Ha.

For the low-Hartmann number *stationary* longitudinal instabilities, in the dominant kinetic energy balance, the production of fluctuating energy by shear of mean flow $\overline{K}_f$ serves as the main destabilizing contribution, which grows with the increased values of Ha. The energy production due to buoyancy forces serves here as the secondary, very weak stabilizing effect with $\overline{K}_b \ll \overline{K}_f$.

In the thermal energy balance both contributions due to temperature transport are destabilizing. At the lowest values of the Hartmann number, the horizontal temperature transport $\overline{\Theta}_2$ term is dominant and decreases with increasing Ha, while previously secondary vertical temperature transport $\overline{\Theta}_1$ contribution increases and takes over as a main destabilizing term.

The ratio R_d decreases with the increasing magnetic field strength, indicating the decreasing influence of dynamical effects.

Summary of transitions of the most dangerous modes at the Hartmann number increases is shown in Tables III and IV for both electrically insulating and conducting walls. The qualitative picture is not changed by the differences in wall conductivities. However, for electrically conducting walls the importance of longitudinal modes diminishes as the transition to the transverse oscillatory mode occurs at lower value of the Hartmann number.

TABLE III. Most dangerous modes, thermally conducting and electrically insulating walls.

instability type	Ha	k_{cr}	f
transverse stationary	$0 \to 8.93$	$2.68 \to 1.51$	0
longitudinal oscillatory	$8.93 \to 38.25$	$2.24 \to 2.43$	$512 \to 4020$
longitudinal stationary	$38.25 \to 46.09$	$21.38 \to 23.6$	0
longitudinal oscillatory	$46.09 \to 148.7$	$10.96 \to 18.96$	$2315 \to 3616$
transverse oscillatory	≥ 148.7	≥ 14.22	≥ 32359

TABLE IV. Most dangerous modes, thermally and electrically conducting walls.

instability type	Ha	k_{cr}	f
transverse stationary	$0 \to 9.09$	$2.68 \to 1.5$	0
longitudinal oscillatory	$9.09 \to 36.31$	$2.37 \to 2.54$	$587.5 \to 4894$
longitudinal stationary	$36.31 \to 45.99$	$21.61 \to 24.21$	0
longitudinal oscillatory	$45.99 \to 85.36$	$12.12 \to 17.55$	$2136 \to 2601$
transverse oscillatory	≥ 85.36	≥ 10.23	≥ 30619

VI. THERMALLY INSULATING WALLS

In the case of thermally insulating boundaries there are no regions of unstable thermal stratification. Thus the Rayleigh-Benard mechanism no longer applies. The results for transverse modes are shown in Fig. 7. For low Ha they are very similar to the case of thermally conducting boundaries as the mode has a dynamic origin. For higher Ha, transverse, oscillatory rolls related to the instability of the Hartmann layers of the basic profile may appear. However, after a careful search we have not found this mode for the values of Gr currently achievable.

For the longitudinal oscillatory mode, changing thermal boundary conditions from conducting to insulating shifts the onset of instability to much lower Grashof numbers, though this mode is more quickly stabilized and disappears at $Ha \approx 21$.

Longitudinal *stationary* curves for both thermally conducting and thermally insulating walls are relatively close to one another, with the insulating case mode being slightly more dangerous for $Ha < 14$ and the conducting case mode for $Ha > 14$.

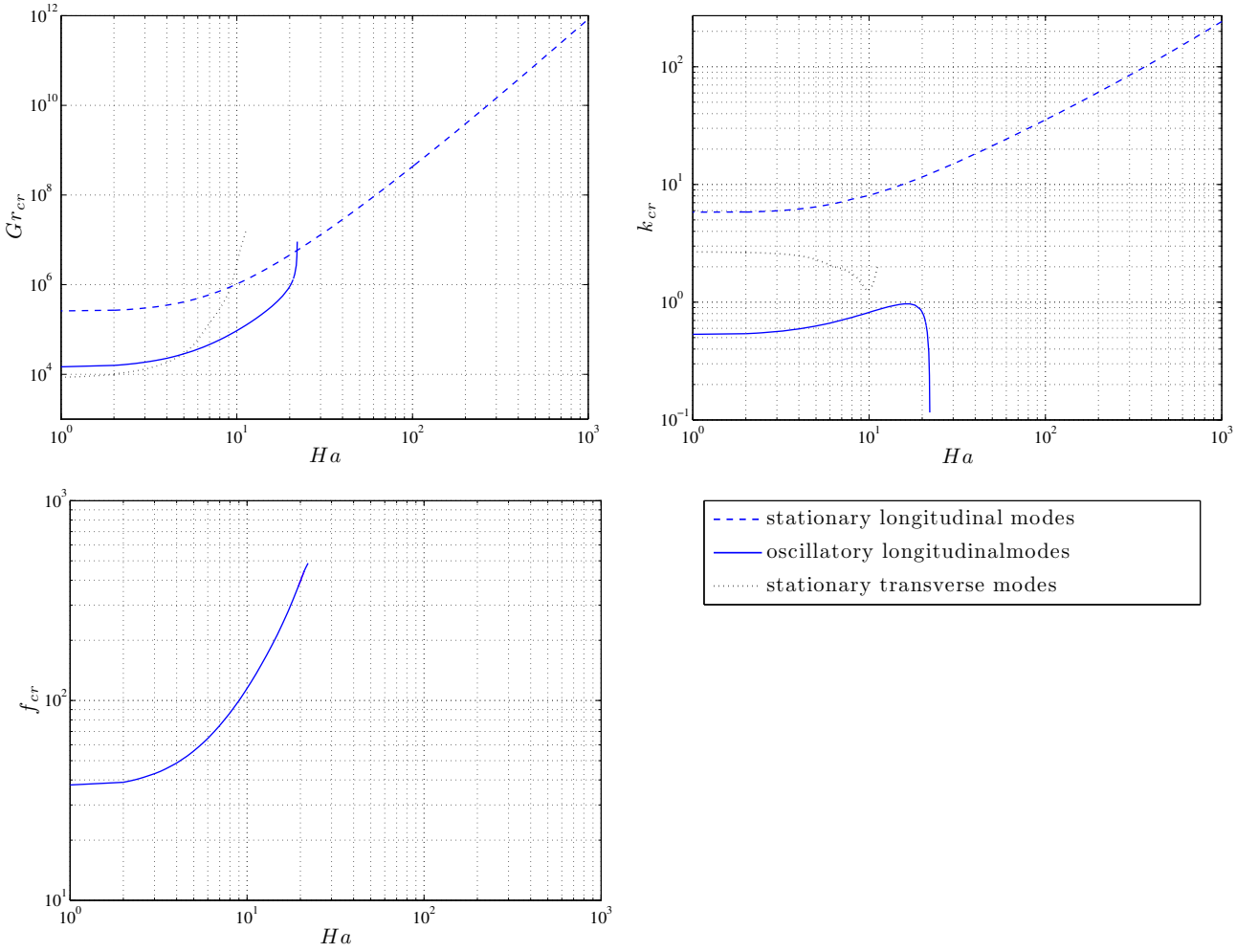

FIG. 7. Critical values of parameters for thermally and electrically insulating walls.

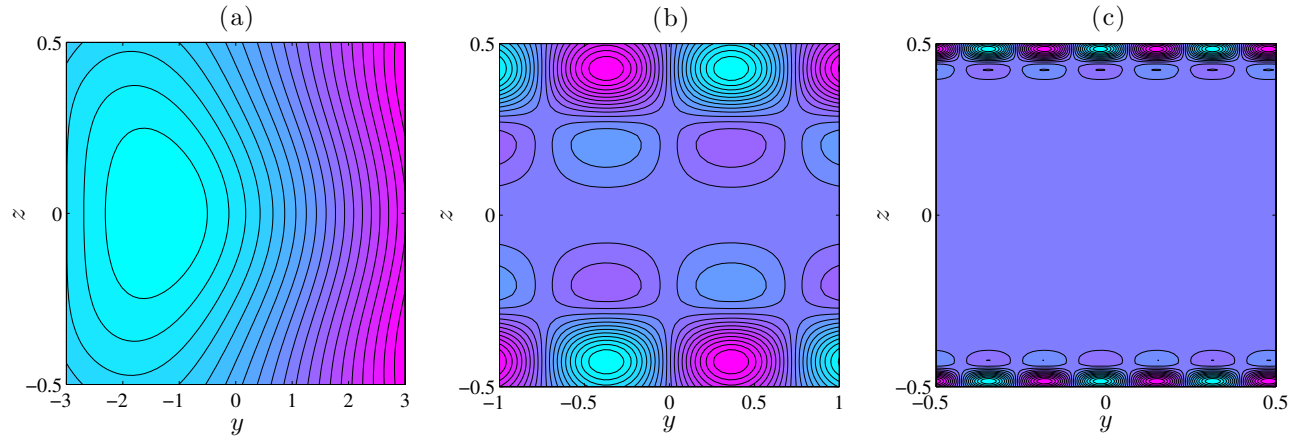

FIG. 8. Disturbance of temperature for the longitudinal oscillatory mode and for $Ha = 10$ ($f_{cr} = 195.2$) (a), and the longitudinal stationary mode for $Ha = 10$ (b), $Ha = 100$ (c). Thermally and electrically conducting walls.

TABLE V. Energy balance for thermally and electrically insulating walls for increasing values of Ha: longitudinal modes.

Ha	$\overline{K}_f$	$\overline{K}_b$	$\overline{K}_m$	$\overline{\Theta}_1$	$\overline{\Theta}_2$	R_d
oscillatory instabilities						
2	0.49	0.60	-0.09	-0.07	1.07	0.29
6	0.69	1.00	-0.69	-0.14	1.14	0.24
10	0.90	1.71	-1.61	-0.29	1.29	0.21
stationary instabilities						
2	1.00	0.01	-0.01	-0.08	1.08	5.69
6	1.07	0.01	-0.08	-0.08	1.08	4.87
10	1.14	0.01	-0.15	-0.10	1.10	3.97
25	1.29	0.02	-0.31	-0.14	1.14	3.18
60	1.39	0.02	-0.41	-0.19	1.19	2.98
100	1.43	0.02	-0.45	-0.22	1.22	3.04
200	1.46	0.01	-0.47	-0.26	1.26	3.31
500	1.46	0.01	-0.47	-0.29	1.29	4.13
1000	1.46	0.00	-0.46	-0.31	1.31	5.22

In the case of three-dimensional *oscillatory* mode, the wavenumber is roughly three times lower for the thermally insulating case and reaches its maximum $k_y \approx 0.96$ at $Ha \approx 17$. This mode occurs here at lower frequency than in the case of thermally conducting boundaries.

Thermal boundary conditions do not strongly affect the dominant fluctuating thermal energy balance (Table V) for the oscillatory instabilities and similar conclusions can be drawn as for the cases of thermally conducting boundaries. The fluctuating kinetic energy balance is here less affected by the magnetic field than for the thermally conducting walls cases.

For the stationary longitudinal instabilities of dynamical origin, the thermal energy balances strongly depend on the thermal boundary conditions. For the thermally insulating walls, the horizontal temperature transport $\overline{\Theta}_2$ is the only destabilizing effect, growing with the increasing Hartmann number Ha. The vertical temperature transport $\overline{\Theta}_1$ serves here as a weak stabilizing contribution, becoming more pronounced at the higher values of Ha.

The dominant kinetic fluctuating energy balance is here very similar to the case of thermally conducting and electrically insulating boundaries. There is one exception here, however. The shear of the basic velocity profile is the main destabilising factor. It is this effect, concentrated in the Hartmann layers that leads to the instability. This is clearly seen in Fig. 8, as with increasing Ha the instability tends to be located at the Hartmann layers. The kinetic contributions are here slightly more influenced by the magnetic field strength,with the stronger respective stabilizing and destabilizing terms.

For the stationary longitudinal mode, and for high values of the Hartmann number, $Ha \sim 10^3$, the critical values of parameters reach asymptotic relations $Gr_{cr} \cong 70.01\, Ha^{3.36}$ and $k_{cr} \cong 0.59\, Ha^{0.87}$.

The summary of the results is presented in Tables VI and VII. Again, the type of electrical boundary conditions does not change the qualitative picture of the transitions, so that at high Ha the longitudinal stationary rolls in the Hartmann layers prevail.

TABLE VI. Most dangerous modes, thermally and electrically insulating walls.

instability type	Ha	k_{cr}	f
transverse stationary	$0 \to 4.94$	$2.68 \to 2.32$	0
longitudinal oscillatory	$4.94 \to 21.34$	$0.63 \to 0.62$	$55.44 \to 449$
longitudinal stationary	≥ 21.34	≥ 12.04	0

TABLE VII. Most dangerous modes, thermally insulating and electrically conducting walls.

instability type	Ha	k_{cr}	f
transverse stationary	$0 \to 5.8$	$2.68 \to 2.11$	0
longitudinal oscillatory	$5.8 \to 17.02$	$0.84 \to 0.55$	$98.86 \to 698$
longitudinal stationary	≥ 17.02	≥ 11.34	0

VII. CONCLUSIONS

Linear stability of a buoyant, magnetohydrodynamic flow in a horizontal fluid layer owing to the horizontal temperature gradient for a low Prandtl number has been considered. The applied magnetic field is vertical and is supposed to be sufficiently strong, characterized by the Hartmann number, $Ha > 10$. The horizontal walls are thermally or electrically conducting or insulating, which leads to four different combinations of the boundary conditions.

It has been shown that there are two main factors strongly affecting the instabilities, namely the type of the thermal conductivity of the walls (conducting or insulating) and the value of the Hartmann number, Ha.

For *thermally conducting* walls as Ha increases from zero the most unstable modes undergo the following transitions: transverse stationary→longitudinal oscillatory→longitudinal stationary→longitudinal oscillatory→transverse oscillatory. For a sufficiently high magnetic field, when the transverse modes of dynamic origin are damped for $Ha \sim 10$, the main source of instability becomes thermal, owing to the unstable thermal stratification in the lower and upper regions of the layer. The asymptotics of the critical parameters for the most unstable modes is $Gr_{cr} \sim Ha^2$, $k_{cr} \sim Ha^{1/3}$, similar to the Rayleigh-Bénard problem[10], i.e. the instabilities consist of narrow cells or rolls. Although this asymptotics is valid for both longitudinal and transverse modes, the latter one is oscillating and is more unstable as it draws energy from the basic flow. The frequency of this mode has the asymptotics $f \sim Ha^{1/3}$.

For *thermally insulating* walls, where no Rayleigh-Bénard mechanism exists, the transitions between the modes is simpler as Ha increases, and is transverse stationary→longitudinal oscillatory→longitudinal stationary. The flow overall is much more stable, with $Gr_{cr} \sim Ha^3$, $k_{cr} \sim Ha$ as $Ha \to \infty$. These are much more narrow than for thermally conducting boundaries, and are at the scale of the Hartmann layers, where the disturbance is concentrated. The most unstable modes, however, are not conventional instability of the Hartmann layer[9], which would occur transverse to the basic flow. The most dangerous instabilities are longitudinal stationary modes and are of combined dynamic-thermal origin and occur owing to high longitudinal shear in the Hartmann layers, which leads to stretching of the isolines of the disturbance temperature in those regions. In fact, the asymptotics of $Gr_{cr} \sim Ha^3$ is very interesting. From Eq. (15) follows that Gr/Ha^2 plays the role of the Reynolds number, Re. Then from Sec. IV follows that the well-known parameter from isothermal MHD flows is Re_{cr}/Ha, which is much lower than Lock's result of $50,000$. In fact, these perturbations resemble the optimal instabilities for the Hartmann layers[11,12].

Of course, in a real horizontal Bridgman crystal growth process, the basic flow is far more complicated. The reason is that the real process occurs in a rectangular box rather than the fluid layer. This brings in quite a complex, three-dimensional basic flow, involving jets at all the walls parallel to the magnetic field[13], including the one at the face of the growing crystal. These jets may become unstable, similar to pressure-driven flows in ducts[14]. Thus this investigation should be considered as an initial step towards understanding the instabilities in complicated industrial processes.

Finally, it should be noted that from a fundamental point of view the problem with thermally conducting boundaries has certain links to the classical magnetoconvection one with zero basic flow, as the source of the instability in both is unstable thermal stratification. In both cases, for sufficiently high values of Ha, the resulting instability structures are narrow rows/cells of thickness $O(Ha^{-1/3})$.[10] For $Pr_m \equiv 0$, both here and in the layer heated from below there is practically no difference between the electrical conductivity of the walls. For a layer, heated from the bottom, new, oscillating modes appear when $Pr_m \neq 0$.[15,16] This is so even if $Pr_m \ll 1$ but still not reaching the values for liquid metals or molten semiconductors, for which $Pr_m \sim 10^{-6}$. These oscillating modes have thermal/Alfvenic origin stemming from bending of the magnetic field lines by the convective flow. For these modes there is a strong dependence of the type of instability on the electrical boundary conditions[15,16]. Similar effects have been found for the problem considered here[17] and will be published in a separate paper.

REFERENCES

[1] H. Ozoe, *Magnetic Convection* (Imperial College Press, 2005).

[2] U. Müller and L. Bühler, *Magnetofluiddynamics in Channels and Containers* (Springer, 2001).

[3] S. Kaddeche, D. Henry, and H. Ben Hadid, "Magnetic stabilization of the buoyant convection between infinite horizontal walls with a horizontal temperature gradient," Journal of Fluid Mechanics **480**, 185–216 (2003).

[4] D. Henry, A. Juel, H. Ben Hadid, and S. Kaddeche, "Directional effect of a magnetic field on oscillatory low-prandtl-number convection," Physics of Fluids **181** (2008).

[5] J. Priede, S. Aleksandrova, and S. Molokov, *Stability of buoyant convection in laterally heated liquid metal layer subject to transverse magnetic field* (Proceedings of the 7th PAMIR Conference, France, 2008).

[6] J. Garandet, T. Alboussiere, and R. Moreau, "Buoyancy driven convection in a rectangular enclosure with a transverse magnetic field," Int. Journal of Heat and Mass Transfer **35**, 741–748 (1992).

[7] G. Gershuni and E. Zhukhovitskii, "Stationary convective flow of an electrically conducting liquid between parallel plates in a magnetic field," JETP **34**, 461–464 (1958).

[8] J. Weideman and S. Reddy, "A matlab differentiation matrix suite," ACM TOMS **26**, 465–519 (2000).

[9]R. C. Lock, "The stability of the flow of an electrically conducting fluid between parallel planes under a transverse magnetic field," Proc. Royal Society of London, Ser. A **233**, 105–125 (1955).
[10]S. Chandrasekhar, *Hydrodynamic and Hydromagnetic Stability*, Dover Books on Physics Series (Dover Publications, 1961).
[11]D. Gerard-Varet, "Amplification of small perturbations in a Hartmann layer," Physics of Fluids **14**, 1458–1467 (2002).
[12]C. Airiau and M. Castets, "On the amplification of small disturbances in a channel flow with a normal magnetic field," Physics of Fluids **16**, 2991–3005 (2004).
[13]S. Aleksandrova and S. Molokov, "Three-dimensional buoyant convection in a rectangular cavity with differentially heated walls in a strong magnetic field," Fluid Dynamics Research **35**, 37 – 66 (2004).
[14]J. Priede, S. Aleksandrova, and S. Molokov, "Linear stability of hunt's flow," Journal of Fluid Mechanics **649**, 115–134 (2010).
[15]M. Takashima, M. Hirasawa, and H. Nozaki, "Buoyancy driven instability in a horizontal layer of electrically conducting fluid in the presence of a vertical magnetic field," International Journal of Heat and Mass Transfer **42**, 1689–1706 (1999).
[16]P. Roberts and K. Zhang, "Thermal generation of alfvn waves in oscillatory magnetoconvection," Journal of Fluid Mechanics **420**, 201–223 (2000).
[17]A. Hudoba, *Instabilities in the buoyant convective flows subject to high magnetic fields* (Ph.D. Thesis, Coventry University, UK, 2015).